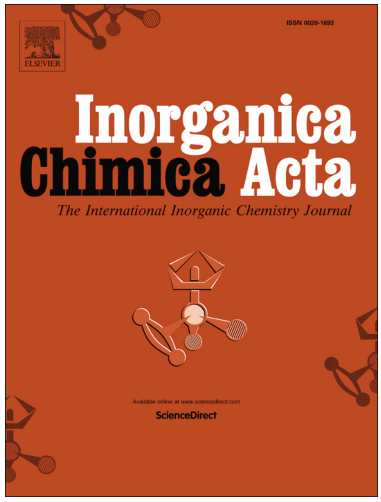

Distinctions of positional isomers of N-(methylthiazol-2-yl)nitrobenzamide by copper and iron ions

Nithi Phukan, Abir Goswami, Jubaraj B. Baruah

PII: S0020-1693(15)00341-2
DOI: http://dx.doi.org/10.1016/j.ica.2015.07.007
Reference: ICA 16600

To appear in: *Inorganica Chimica Acta*

Received Date: 19 June 2015
Revised Date: 12 July 2015
Accepted Date: 13 July 2015

Please cite this article as: N. Phukan, A. Goswami, J.B. Baruah, Distinctions of positional isomers of N-(methylthiazol-2-yl)nitrobenzamide by copper and iron ions, *Inorganica Chimica Acta* (2015), doi: http://dx.doi.org/10.1016/j.ica.2015.07.007

Distinctions of positional isomers of N-(methylthiazol-2-yl)nitrobenzamide by copper and iron ions

Nithi Phukan, Abir Goswami, Jubaraj B. Baruah*
Department of Chemistry, Indian Institute of Technology Guwahati, Guwahati 781 039, Assam, India. Fax: +91-361-2690762; Ph. +91-361-2582311; email: juba@iitg.ernet.in; url: http://www.iitg.ernet.in/juba.

Abstract: The fluorescence emissions of six positional isomers of N-(methylthiazol-2-yl)-nitrobenzamide are selectively reduced upon interactions with Cu^{2+}, Fe^{2+} or Fe^{3+} ions among various metal ions that were studied. One isomer, namely N-(4-methylthiazol-2-yl)-3-nitrobenzamide shows reduction in the fluorescence emission intensity only upon interactions with Fe^{2+} or Fe^{3+} ions, enabling detection of the iron ions. Specific fluorescence emissions changes observed were used to distinguish N-(4-methylthiazol-2-yl)-3-nitrobenzamide from the other structural isomers of this compound. The positional isomers of the N-(4-methylthiazol-2-yl)-3-nitrobenzamide are difficult to distinguish at low concentrations by using other conventional techniques. On the basis of the evidences obtained from the lifetime measurements and the ESR studies, selective discrimination of Cu^{2+} ions by this particular isomer is explained on the basis of the metal complex formation by the other positional isomers with Cu^{2+} ions other than this isomer, such metal complexation influence the internal charge transfer processes.

Key words: Thiazoles; Positional isomers; Fluorescence; Copper and Iron ions.

Introduction:

Sensing of metal ions by various polydenate ligands [1-2] and the analytical chemistry of metal ions with small molecules as analytes have relevance in present-day research [3-5]. Such research works stem from selective interactions of organic substrates with one or more metal ions which are generally influenced by position as well as the nature of the functional group/s on the organic moiety. Hence, there is an avenue to screen positional isomers of organic molecules of similar backbones. Nuclear magnetic resonance [6] or mass spectroscopy [7-8] generally distinguishes positional isomers; but such methods require high-end equipment. From a supramolecular chemistry point of view, proton-transfer between constituents of a host-guest complex [9-11] can be used to visually identify positional isomers. Due to high sensitivity with fast and thorough output of fluorescence emission of fluorescent substrates upon interaction with metal ions, fluorescence turning *on* and *off* is a conventional signal transduction technique to differentiate analytes [12-16]. The intensity and position of fluorescence emission are guided by various mechanisms, hence it also provides avenue to design receptors to operate through a definite path [15-16]. The role of an organogel matrix in the capabilities of colorimetric sensing of positional isomers of hydroxy-aromatics was demonstrated by Shinkai and his coworkers [17]. On the other hand, capabilities of different anionic templates of positional isomers of polyaromatic sulphonates to recognize nucleobases were revealed by Ward and his group [18]. Suslick and his coworkers elucidated utilities colorimetric and fluorometric sensor arrays to discriminate similar analytes with high sensitivity [19]. In spite

Figure 1 here

of emerging literature and methodologies in the analytical chemistry of metal ions there is no concerted literature [20] in which selective interactions of multiple metal ions toward organic positional isomers have been studied. Such an approach may be considered as bio-inspired, as many enzymes selectively bind certain metal ions, in which the binding modes are also very specific [21-23]. We set our study to distinguish a set of isomers that have donor and acceptor units tethered through an amide linkage which would show fluorescence emission via an internal charge transfer mechanism as illustrated in figure 1. Additionally the excited state would be highly sensitive to interacting metal ions where a subtle difference would cause a

change in emission features. In such cases interference of a metal ion with the excited or ground state population would help to modulate the intensity of such fluorescence processes.

Figure 2 here

We have chosen six new positional isomers of N-(methylthiazol-2-yl)nitrobenzamide shown in Figure 2 for such a study. The choice of these isomers is based on the fact that thiazole unit is an important constituent of medicinal compounds such as vitamin B_1 [24], cystothiazole A [25] and sulfathiazole [26]. Thiazole derivatives are constituents of polymeric materials [27], liquid crystals [28], photonucleases [29], fluorescent dyes [30-31], insecticides [32] and biologically active molecules [33-34].

Experimental:

General:

^{1}H-NMR spectral data were recorded on Varian-AS400 spectrometers. UV-vis spectral data were recorded using a Perkin-Elmer Lambda 750 UV-vis spectrophotometer. Fluorescence measurements were performed on Fluoromax-4 spectrofluorometer using 10 mm path length quartz cuvettes with a slit width of 10 nm at room temperature. Time-resolved fluorescence decays were measured on a picosecond time-resolved cum steady state luminescence spectrometer, Eddinburg Instrument model: FSP920. Infrared spectra were obtained by using a Perkin-Elmer FT-IR spectrophotometer (4000-400 cm^{-1}). ESI-mass spectra were recorded on a micro mass Q-TOF (Waters) mass spectrometer using an acetonitrile / formic acid matrix. ESR spectra were run on a JEOL, Model: JES-FA200 ESR spectrometer. Energy level calculations were carried out in Gaussian03W using density functional theory with a hybrid B3LYP functional and the 6-31++g (d,p) basis set.

Synthesis and characterisation:

The compounds $\mathbf{L^1}$ and $\mathbf{L^2}$ were prepared by reacting 3-nitrobenzoyl chloride with the corresponding isomer of 2-amino-methyl thiazole. Similarly for the $\mathbf{L^3}$ and $\mathbf{L^4}$ 2-nitrobenzoyl chloride and for the $\mathbf{L^5}$ and $\mathbf{L^6}$ 4-nitrobenzoyl chloride were used in place of 3-nitrobenzoyl chloride. In a typical experiment 3-nitrobenzoyl chloride (0.185 g, 1 mmol) was dissolved in dichloromethane (20 mL) under nitrogen atmosphere.

Solution was cooled to 0 °C by placing on an ice-bath and 2-amino-5-methylthiazole (0.114 g, 1 mmol) was added to the reaction mixture. It was stirred overnight. A white precipitate of N-(5-methylthiazol-2-yl)-3-nitrobenzamide (**L^1**) was obtained, which was filtered, washed with water and dried in vacuum. Yield, 0.240g (92%). ^{1}H-NMR (400MHz, DMSO-d_6): 8.65 (s, 1H), 8.48 (d, 9.2 Hz, 1H), 8.36 (d, 7.6 Hz, 1H), 7.91(t, 8.0Hz, 1H), 7.20 (s, 1H), 6.60 (s, 1H), 2.09 (s, 3H). Mass (ESI): Cacld m/z for $C_{11}H_9N_3O_3S$, 263.0365; found (m+1), 264.0445. IR (KBr, cm^{-1}): 3458 (w), 3092 (m), 1669 (m), 1614 (m), 1533 (s), 1436 (m), 1343 (s), 1152 (m), 1070 (m), 917 (s), 714 (s), 514 (m). Crystallographic parameters: Crystal system, Monoclinic; Space group, $P2_1/n$; a(Å), 3.9164(5); b(Å), 13.1518(12); c(Å), 22.183(3); α = β(°), 90.00; γ(°), 94.628(11); V(Å^3), 1138.9(2); Z, 4; Density ($g.cm^{-3}$), 1.535; Abs. Coeff. (mm^{-1}), 0.288; Abs. Correction, multi-scan; F (000), 544; Total reflections, 2008; Reflections, $I > 2\sigma(I)$, 1164; Max. θ/°, 25.00; Ranges (h, k, l), $-4 \le h \le 4$, $-9 \le k \le 15$, $-26 \le l \le 11$; Completeness to 2θ (%), 99.9; Data/ restrain/ parameter; 2008/0/164; Goof, 1.005; R indices [$I>2\sigma(I)$], 0.0594; R indices (all data), 0.1144.

Yields and spectroscopic details of compounds **L^2**-**L^6** are listed below:

N-(4-methylthiazol-2-yl)-3-nitrobenzamide (**L^2**): Pale yellow solid; Yield 0.246g (94%); ^{1}H-NMR (400MHz, DMSO-d_6): 8.62 (s, 1H), 8.48 (d, 9.2 Hz, 1H), 8.36 (d, 7.6 Hz, 1H), 8.31 (s, 1H), 6.26 (s, 1H), 2.09 (s, 3H). ESI mass (m/z) 264.0459 (m+1). IR (KBr, cm^{-1}): 3445 (w), 3109 (s), 1712 (s), 1645 (m), 1522 (s), 1430 (s), 1370 (s), 1343 (s), 1224 (s), 1152 (m), 1072 (s), 948 (m), 823 (m), 788 (m), 720 (s), 583 (s).

N-(5-methylthiazol-2-yl)-2-nitrobenzamide **(L^3)** Yield 0.247g (94%); ^{1}H-NMR (400MHz, DMSO-d_6): 8.44 (d, 9.6 Hz, 1H), 8.07 (d, 7.2 Hz, 1H), 7.97 (t, 8.4 Hz, 1H), 7.86 (t, 6.8 Hz, 1H), 7.05 (s, 1H), 2.21 (s, 3H). ESI-mass (m/z) 264.0445 (m+1). IR (KBr, cm^{-1}): 3387 (w), 3268 (w), 3093 (w), 1630 (s), 1586 (s), 1361 (m), 1148 (w), 910 (m), 796 (s), 704 (s), 593 (w).

N-(4-methylthiazol-2-yl)-2-nitrobenzamide (**L^4**): Yield, 0.240g (90%); ^{1}H-NMR (400MHz, DMSO-d_6): 8.44 (d, 9.6 Hz, 1H), 8.07 (d, 7.2 Hz, 1H), 7.97 (t, 8.4 Hz, 1H), 7.86 (t, 6.8 Hz, 1H), 7.05 (s, 1H), 2.21 (s, 3H). ESI-mass (m/z): 264.0445 (m+1). IR (KBr, cm^{-1}): 3443 (w), 3317 (m), 3095 (w), 1659 (s), 1620 (s), 1582 (s), 1431 (m), 1388 (m), 782 (s), 722 (s), 633 (m), 536 (s).

N-(5-methylthiazol-2-yl)-4-nitrobenzamide **(L^5)**: Yield, 0.223g (85%); ^{1}H-NMR (400MHz, DMSO-d_6): 8.28 (d, 8.0 Hz, 2H), 8.23 (d, 8.4 Hz, 2H), 7.20 (s, 1H), 2.27 (s, 3H). ESI-mass

(m/z): 264.0445 (m+1). IR (KBr, cm^{-1}): 3448 (w), 2924 (s), 2842 (m), 1687 (m), 1641 (m), 1518 (m), 1345 (s), 1261 (s), 1102 (m), 1015 (s), 803 (s), 717 (s).

N-(4-methylthiazol-2-yl)-4-nitrobenzamide (**L^6**): Yield, 0.228g (87%); ^{1}H-NMR (400MHz, DMSO-d_6): 8.18 (d, 9.2Hz, 2H), 8.13 (d, 9.6Hz, 2H), 6.20 (s, 1H), 2.47 (s, 3H). Mass (ESI) found m/z: 264.0445 (M+1), IR (KBr, cm^{-1}): 3448 (w), 1698 (w), 1541 (m), 1431 (m) 1348 (m), 1180 (m), 1036 (s), 921 (s), 860 (s), 800 (s), 717 (s).

Results and Discussion:

A series of new positional isomers shown in Figure 2 were synthesized by reacting two isomers of 2-amino-methylthiazole with corresponding nitrobenzoyl chloride and were characterised by common spectroscopic techniques.

Study on the fluorescence emission changes of isomers have shown that independent solution of each of **L^1**-**L^6** in dimethylformamide (DMF) or in aqueous DMF (30%) shows absorption maxima at ~275 nm and all these compounds show fluorescence emissions in the range of 400-415 nm on excitation at 280 nm. For example, **L^1** in DMF shows fluorescence emission at 410 nm when excited at 280 nm, whereas similar excitation causes broad fluorescence emission at 405 nm for **L^2**. Thus these isomers are difficult to distinguish from their individual emission spectra or from absorption spectra. Fluorescence emission occurring at longer wavelengths on excitation at shorter wavelength arises due to internal charge transfer (ICT) and this phenomenon was observed in thioimidazole tethered to electron accepting units [35].

Figure 3 here

To confirm the feasibility of involvement of charge transfer processes contributing to the fluorescence changes, we have carried out energy calculations of each isomer using the density functional theory package in Gaussian03W. We observed that the energy difference between **L^1** and **L^2** are 1.44 kcal/mole, the HOMO and LUMO of these two compounds visualized with GaussView have shown that the HOMO in these molecules are localized over the thiazole ring, whereas the LUMO is localized at the nitrobenzene ring which is relatively less electron-rich than the thiazole ring (Figure S11). Analysis of the other four isomers **L^3**-**L^6** have established the in these cases also HOMO and LUMO are localised in a similar to the **L^1** or **L^2**. Thus, the emissions

occurring in these isomers are attributed to the charge transfer occurring upon excitation from the HOMO to LUMO.

Table 1 here

Since these isomers could not be distinguished easily from their respective fluorescence emissions, the effects of various chloride salts of metal ions such as Zn^{2+}, Cd^{2+}, Co^{2+}, Pb^{2+}, Ni^{2+}, Cu^{2+}, Fe^{3+}, Al^{3+}, Cr^{3+}, Hg^{2+}, Ag^{+}, Mg^{2+}, Ba^{2+}, Mn^{2+}, Na^{+}, K^{+}, Ca^{2+}, and the sulphate salt of Fe^{2+} with compounds $\mathbf{L^1}$-$\mathbf{L^6}$ were studied by using steady-state fluorescence spectroscopy. As an illustrative example, the gradual decrease observed in the fluorescence emission intensity on addition of Cu^{2+} ions to a solution of $\mathbf{L^1}$, without a shift in the emission maximum, Figure 3a. Bar graphs showing the relative intensity upon the addition of equimolar amounts of different metal ions to solutions of $\mathbf{L^1}$-$\mathbf{L^6}$ are shown in Figures 3b-3f. We also found that fluorescence emission of $\mathbf{L^2}$ was not affected by metal ions that were tested with $\mathbf{L^1}$ with the exception of the Fe^{2+} or Fe^{3+} ions. Thus, the specific fluorescence change of compound $\mathbf{L^2}$ towards Fe^{2+} or Fe^{3+} ions provided an easy way to differentiate two positional isomers. Two isomers having identical nitrobenzamide motifs, but a methyl group at different positions of the thiazole ring, for example, positional isomers, $\mathbf{L^1}$ and $\mathbf{L^2}$ showed similar UV-visible absorption maximum at 270 nm. Addition of copper(II) chloride or iron(III) chloride to a solution of $\mathbf{L^1}$ or $\mathbf{L^2}$ showed an increase in intensity of their respective absorption at 270 nm, hence these two isomers could not be distinguished by UV-visible spectra but this experiment suggested that $\mathbf{L^1}$ and $\mathbf{L^2}$ bind to these metal ions.

The binding constants of each isomer with the interacting metal ion were determined by using a Benesi-Hildebrand plot; the data are listed in Table 1. The relative magnitudes of logarithm of binding constants fall between ~3.4-5.3 suggesting that the logK values are comparable. Since the structures of positional isomers are based on three closely related structures, one would expect similar binding constants of the isomers having similar methylthiazole part, which was not observed. In present examples, a correlation of structures of the isomers with the binding constants with a metal ion is not possible. On the other hand, binding constants with iron do not help to distinguish the isomers in a definitive manner. Thus, the non-observation of changes in intensity of the fluorescence of $\mathbf{L^2}$ by Cu^{2+} ions becomes the distinguishing factor of $\mathbf{L^2}$ from the other positional isomers. The observations

on the Fe^{2+} and Fe^{3+} ions effectively quenching the fluorescence of all the ligands and Cu^{2+} ions quenching the fluorescence of all but the **L²** ligand suggest that such quenching processes are not due to the simple effect of the paramagnetic species alone but supports an quenching process passing through ICT mechanism as elucidated in the Figure 1. Cu^{2+} ions failed to quench the fluorescence of the **L²**, hence we could not calculate a binding constant in this case. As effective quenching requires metal-ligand interactions, it may be suggested that there is no effective complex formation between **L²** and Cu^{2+} ions. Paramagnetic ions such as Mn^{2+} ions failed to quench fluorescence emissions of these ligands, which suggested that there must be definite metal-ligand interactions to show quenching of the fluorescence emissions.

Table 2 here

Fluorescence emission of **L¹** at 410 nm has lifetime of 9.34 ns, which slightly changes in the presence of Fe^{3+} or Cu^{2+} ions. In the presence of Fe^{3+} it is 8.57 ns, whereas in the presence Cu^{2+} it is biexponential and the major fraction has a lifetime 8.07 ns. On the other hand, **L²** shows biexponential lifetime, and the addition of copper ions lowers the lifetime. It was not possible to determine lifetime from equimolar concentrations of Fe^{3+} and ligand **L²**, but it was determined at a thousand-fold lower ratio of Fe^{3+} with respect to the ligand. In this case we observe insignificant change in lifetime from the pure ligand. Thus, the quenching effect of Cu^{2+} ions in this case is significantly less than that of the Fe^{3+} ions. Despite the fact that the copper ions quench the fluorescence, it does not have a slight effect on the life-time of the process. The observed changes in fluorescence, which are due to the interaction of the ligand with a metal ion, not only affect the emission lifetime, but also the probability of ICT transitions.

The crystal structure of **L¹** shows (Figure 4) a non-planar structure, in which the sulphur atom of the thiazole ring and the oxygen atom of amide project toward the same side of the structure. Although there are examples in the literature of thiazole copper complexes having distorted octahedral geometry [36], we could not get crystalline copper or iron complexes from reaction with any of the ligands. From Job plots determined from absorption changes in the UV region we find that **L¹** and **L²**

Figure 4 here

forms a copper complex in 1: 4 metal:ligand ratio in solution (Figure S16). These ligands are not planar, hence their respective copper complexes could be formed by the coordination of two bidentate ligands coordinating through nitrogen atom of thiazole and the nitrogen atom of amide to form four-member chelate, and two mono-dentate ligands (along the z-axis) binding through their thiazole nitrogen atoms. We tried to get crystals of complexes from reactions of the ligands with copper and iron salts in acetonitrile and alcohol which was not successful.

We observed ESR signals from a solution of **L^1** in dimethylformamide (DMF) with cupric chloride at $g_{//} = 2.117$ and $g_{\perp} = 2.066$ (Figure S17). Whereas, a solution of equimolar **L^2** and cupric chloride in DMF has a broad ESR signal at g = 2.170, which is identical to a solution of cupric chloride in DMF. It is observed that $g_{//} > g_{\perp}$ in the former case, which suggests that unpaired electron resides in the dx^2-y^2 -orbital of copper ion whereas in the later unpaired electron occupies dz^2-orbital [37]. It may be mentioned that each HOMO (Figure S10) of ligands **L^1-L^6** has symmetry appropriate to interact with dx^2-y^2 orbital. ESR experiments suggest that among the **L^1** and **L^2** only the **L^1** forms complex with Cu^{2+}ions. This is consistent with the lack of quenching observed in the Cu^{2+}-**L^2** mixture. Dihedral angles of amide bonds may influence internal charge transfer [38-39], but in our case we find that such differences are not important in this set of compounds because the optimized geometry of the isomers do not show significant differences.

Conclusions:

Based on a design principle stemming from an internal charge transfer mechanism, it is shown that interactions of Fe^{2+} or Fe^{3+} ions result in drastic decrease in the fluorescence emission intensity of **L^1-L^6** which does not happen in the presence of many other common metal ions. The fluorescence emission changes caused on **L^2** are very specific to Fe^{2+} or Fe^{3+} ions. Among the **L^1-L^6** isomers **L^1**, **L^3-L^6** also show a decrease in fluorescence intensity upon addition of Cu^{2+} ions, but the fluorescence emission of **L^2** is unaffected by Cu^{2+} ions. Such an exceptional recognition of one positional isomer among six isomers by ions of two of the most abundant transition metal ions present in humans and mammals provides a rationale to screen many other isomeric systems by fluorescence technique which may be difficult to distinguish by other spectroscopic tools.

Acknowledgments:

Author N.P. thanks Council of Scientific and Industrial Research, New Delhi, India, for a Senior Research Fellowship.

Supporting information: Spectroscopic details and fluorescence measurement plots are available. The CCDC deposition number for the CIF of $\mathbf{L^1}$ is 1058371.

References:

1. J. Lei, R. Qian, P. Ling, L. Cui, H. Ju, Trends in Anal. Chem., 55 (2014) 71-78.
2. X. Zhao, X. Bu, T. Wu, S. -T. Zheng, L. Wang, P. Feng, Nature Commun., 4 (2013) 2344.
3. B. Valeur, I. Leray, Coord. Chem. Rev., 205 (2000) 3-40.
4. S. Pal, N. Chatterjee, P. K. Bharadwaj, RSC Adv., 4 (2014) 26585-26620.
5. X. Chen, T. Pradhan, F. Wang, J. S. Kim, J. Yoon, Chem. Rev., 112 (2012) 1910-1956.
6. Z. Szafran, J. Chem. Edu., 62 (1985) 260-261.
7. F. Hsu, J. Turk, M. L. Gross, J. Mass Spect., 38 (2003) 447-457.
8. K. Jiang, G. Bian, Y. Pan, G. Lai, Int. J. Mass Spec., 299 (2011) 13-19.
9. D. Kalita, J. B. Baruah, J. Mol. Struct., 969 (2010) 75-82.
10. D. Kalita, J. B. Baruah, J. Chem. Sci., 125 (2013) 267-273.
11. B. R. Jali, J. B. Baruah, ChemPlusChem, 78 (2013) 589-597.
12. A. P. de Silva, T. S. Moody, G. D. Wright, Analyst, 134 (2009) 2385-2393.
13. P. Ceroni, V. Balzani in The exploration of supramolecular systems and nanostructures by photochemical techniques. P. Ceroni, Ed.; ch. 2; Springer, 2012.
14. J. J. R. Fausto da Silva and R. J. P. Williams, in The Biological Chemistry of the Elements, Oxford University Press, 1992.
15. A. P. de Silva, H. Q. N. Gunaratne, T. Gunnlaugsson, A. J. M. Huxley, C.P. McCoy, J. T. Rademacher, T. E. Rice, Chem Rev., 97 (1997) 1515-1566.
16. L. Prodi, F. Bolletta, M. Montalti, N. Zaccheroni, Coord. Chem. Rev., 205 (2000) 59-83.
17. P. Mukhopadhyay, Y. Iwashita, M. Shirakawa, S. -I. Kawano, N. Fujita, S. Shinkai, Angew. Chem. Int. Ed., 45 (2006) 1592-1595.
18. K. T. Holman, M. D. Ward, Angew. Chem. Int. Ed., 39 (2000) 1653-1656.
19. J. R. Askim, M. Mahmoudia, K. S. Suslick, Chem. Soc. Rev., 42 (2013) 8649-8682.
20. B. R. Jali, J. B. Baruah, Dyes and Pigments, 110 (2014) 56-66.
21. K. J. Waldron, J. C. Rutherford, D. Ford, N. J. Robinson, Nature, 460 (2009) 823-830.

22. W. Kaim and B. Schwederski, in Bioinorganic Chemistry: Inorganic Elements in the Chemistry of Life, Wiley, Chichester, 1994.
23. B. L. Vallee and D. S. Auld, Acc. Chem. Res., 26 (1993) 543-551.
24. M. E. Webb, A. Marquet, R. R. Mendel, F. Rebeille, A. G. Smith, Nat. Prod. Rep., 24 (2007) 988-1008.
25. Y. Suzuki, M. Ojika, Y. Sakagami, R. Fudou, S. Yamanaka, Tetrahedron, 54 (1998) 11399-11404.
26. A. Kleemann, J. Engel, B. Kutscher, D. Reichert, Pharmaceutical Substances: Syntheses, patents, applications. 4th Eds. Georg Thieme Verlag, Stuttgart 2000.
27. L. Y. Wang, C. X. Zhang, Z. Q. Liu, D. Z. Lio, Z. H. Jang, S. P. Yan, Inorg. Chem. Comm., 6 (2003) 1255-1258.
28. A. H. Al-Dujali, A. T. Atto, A. M. Al-Kurde, Eur. Polymer J., 37 (2001) 927-932.
29. Y. Li, Y. Xu, X. Qian, B. Qu., Tetrahedron Lett., 45 (2004) 1247-1250.
30. I. Tintcheva, V. Maximova, T. Deligeorgiev, D. Zaneva, I. Ivanov, J. Photochem. Photobiol. A: Chem., 130 (2000) 7-17.
31. V. C. Rucker, S. Foister, C. Melander, P. B. Dervan., J. Am. Chem. Soc., 125 (2003) 1195-1202.
32. Q. Wang, H. Li, Y. Li, R. Huang, J. Agric. Food Chem., 52 (2004) 1918-1922.
33. B. F. Abdel-Wahab, H. A. Abdel-Aziz, E. M. Ahmed, Eur. J. Med. Chem., 44 (2009) 2632-2635.
34. B. S. Dawane, S. G. Konda, G. G. Mandawad, B. M. Shaikh, Eur. J. Med. Chem., 45 (2010) 387-396.
35. A. Helal, S. H. Kim, H. -S. Kim, Tetrahedron, 66 (2010) 9925-9929.
36. W. J. Eilbeck, F. Homes, A. E. Underhill, J. Chem. Soc. A, (1967) 757-761.
37. E. Garribba, G. Micera, J. Chem. Edu., 83 (2006) 1229-1232.
38. Y. Toriumi, A. Kasuya, A. Itai, J. Org. Chem., 55 (1990) 259-263.
39. H. Kagechika, T. Himi, E. Kawachi, K. Shudo, J. Med. Chem., 32 (1989) 2292-2296.

Figures and Tables:

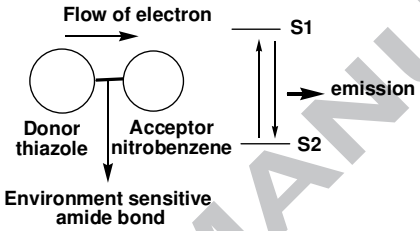

Figure 1: A design principle to screen positional isomers.

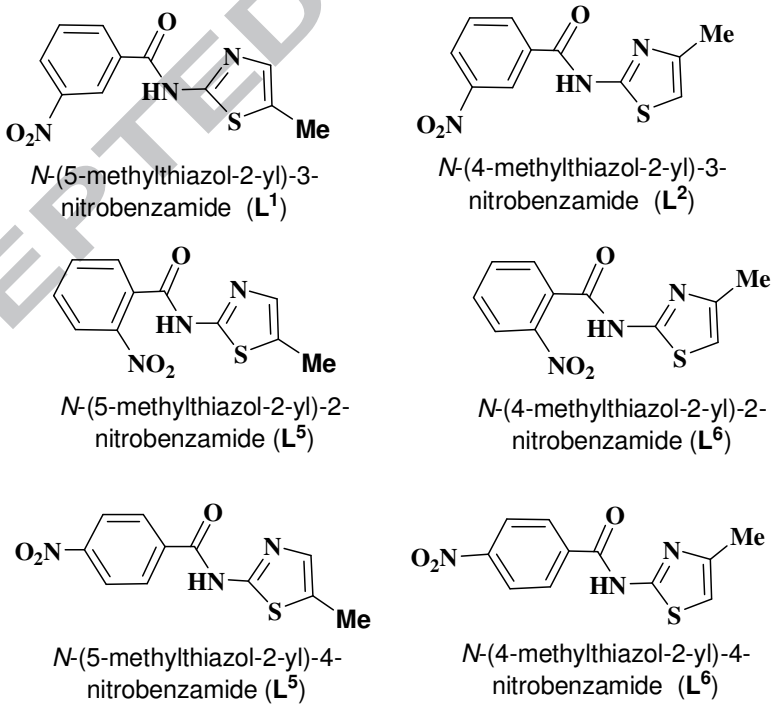

Figure 2: Positional isomers of N-(methylthiazol-2-yl)nitrobenzamide

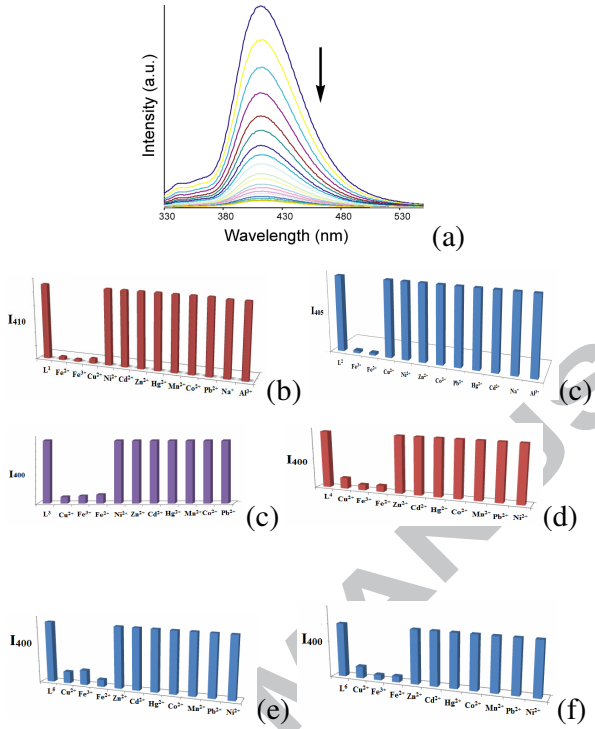

Figure 3: (a) Changes in fluorescence of **L**^{1} (3 mL, 1 × 10^{-4} M in DMF, λ_{ex} = 280 nm) on addition of Cu^{2+} ions (1 × 10^{-2} M). Bar diagrams showing relative fluorescence emission intensity of (b) **L**^{1} at λ_{em} = 410 nm and (c) **L**^{2} at λ_{em} = 405 nm and (c-f) are that of **L**^{3}, **L**^{4}, **L**^{5} and **L**^{6} respectively in presence of various metal ions. I_{400} = normalised emission intensity with respect to the lowest emission intensity.

Table 1: Binding constants with iron and copper ions[#]

Compound	Metal ion	Binding constant (M^{-1})	logK
$\mathbf{L^1}$	Fe^{3+}	6.756×10^3	3.829
$\mathbf{L^1}$	Fe^{2+}	2.024×10^3	5.306
$\mathbf{L^1}$	Cu^{2+}	7.871×10^3	3.895
$\mathbf{L^2}$	Fe^{3+}	2.967×10^4	4.472
$\mathbf{L^2}$	Fe^{2+}	2.087×10^4	4.319
$\mathbf{L^3}$	Fe^{3+}	9.532×10^3	3.979
$\mathbf{L^3}$	Fe^{2+}	9.801×10^3	3.991
$\mathbf{L^3}$	Cu^{2+}	1.3252×10^4	4.122
$\mathbf{L^4}$	Fe^{3+}	1.064×10^4	4.026
$\mathbf{L^4}$	Fe^{2+}	1.291×10^4	4.111
$\mathbf{L^4}$	Cu^{2+}	7.299×10^3	3.863
$\mathbf{L^5}$	Fe^{3+}	$3.4\,01 \times 10^3$	3.532
$\mathbf{L^5}$	Fe^{2+}	7.518×10^3	3.876
$\mathbf{L^5}$	Cu^{2+}	3.436×10^3	3.536
$\mathbf{L^6}$	Fe^{3+}	5.882×10^3	3.769
$\mathbf{L^6}$	Fe^{2+}	7.042×10^3	3.847
$\mathbf{L^6}$	Cu^{2+}	2.724×10^3	3.435

in all cases chloride salts are used for Cu^{2+} and Fe^{3+}, whereas sulphate salt of Fe^{2+} was used. (to avoid oxidation to Fe^{3+} the solution was purged nitrogen gas).

Table 2: Fluorescence lifetime of $\mathbf{L^1}$ and $\mathbf{L^2}$ in the presence of metal ions.

Compound + metal ion	Life time in ns (fraction)
$\mathbf{L^1}$	9.338 (100 %)
$\mathbf{L^1}$ + Fe^{3+}	8.857 (100 %)
$\mathbf{L^1}$ + Cu^{2+}	8.070 (93.3 %) 0.700 (6.7 %)
$\mathbf{L^2}$	7.935 (82.14 %) 1.194 (17.86%)
$\mathbf{L^2}$ + Fe^{3+*}	7.935 (82.51 %) 1.044 (17.49 %)
$\mathbf{L^2}$ + Cu^{2+}	7.305 (83.45 %) 0.945 (16.55 %)

Equimolar concentration of ligand and metal ions.
*at 10^3-times lower concentration of Fe^{3+} with respect to $\mathbf{L^2}$.

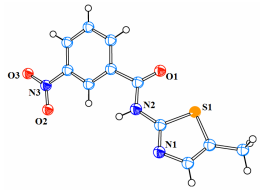

Figure 4: Structure of $\mathbf{L^1}$ (thermal ellipsoids at 50% probability).

Supplementary Information

Distinctions of positional isomers of N-(methylthiazol-2-yl)nitrobenzamide by copper and iron ions

Nithi Phukan, Abir Goswami, Jubaraj B. Baruah*

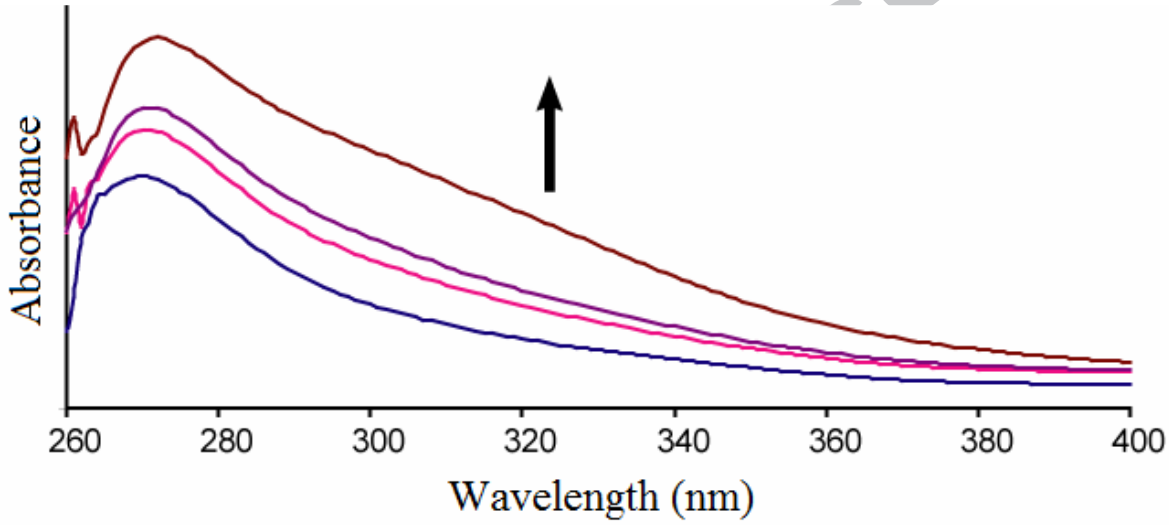

Figure S1: UV–visible spectra of $\mathbf{L^1}$ in dimethylformamide (3ml, 1×10^{-4} M, λ_{max} 270 nm) with Fe^{3+} ions solution added 10µl aliquots.

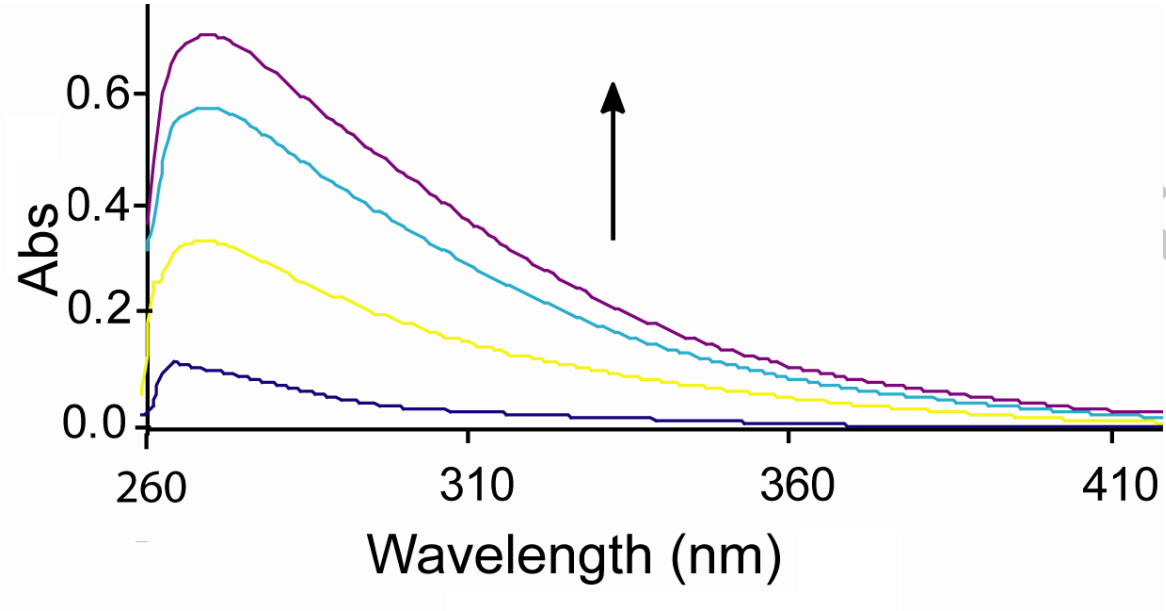

Figure S2: UV–visible spectra of $\mathbf{L^1}$ in dimethylformamide (3 ml, 1×10^{-4} M, λ_{max} 270 nm) with Cu^{2+} ions solution added 10µl aliquots.

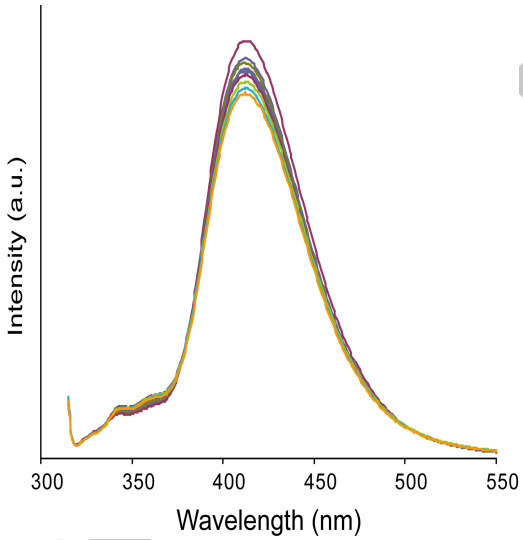

Figure S3: Fluorescence spectra of $\mathbf{L^1}$ in the presence of different metal ions such as Ni^{2+}, Co^{2+}, Zn^{2+}, Cd^{2+}, Hg^{2+}, Mn^{2+}, Al^{3+} and Pb^{2+}.

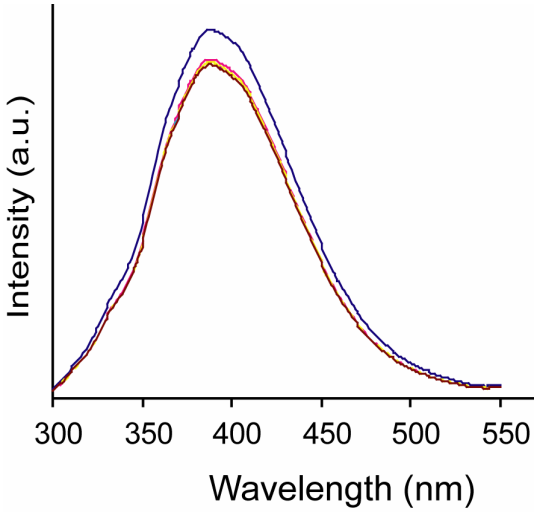

Figure S4: A representative spectra of Fluorescence spectra of $\mathbf{L}^2$ in presence of Ni^{2+} ions to suggest no changes in fluorescence (Similar spectra were observed for all metal ions, except Fe^{2+} and Fe^{3+})

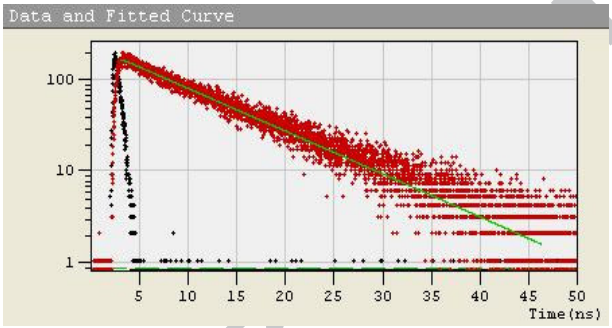

Figure S5: Time-resolved fluorescence decay of $\mathbf{L}^1$ (10^{-5} M in DMF) (ex = 300 nm).

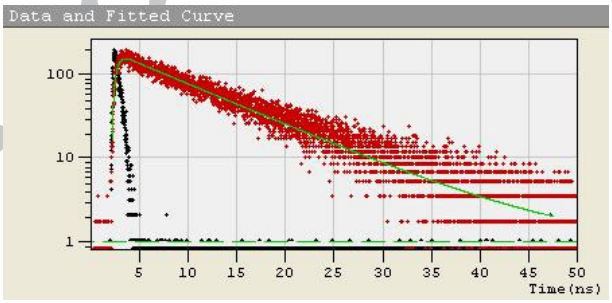

Figure S6: Time-resolved fluorescence decay of L^1-Fe^{3+} system (10^{-5} M in DMF/water, 3:1,v/v) (ex = 300 nm).

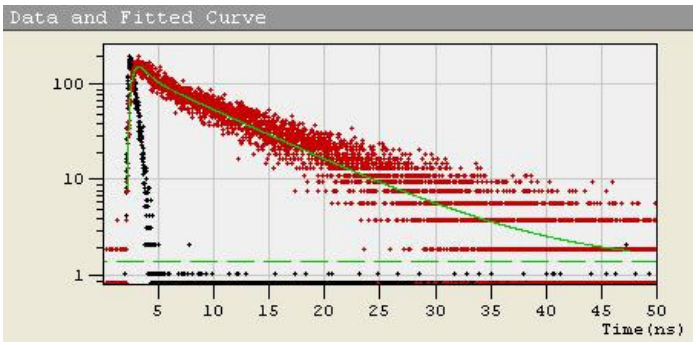

Figure S7: Time-resolved fluorescence decay of L^1-Cu^{2+} system (10^{-5} M in DMF/water, 3:1,v/v) (ex = 300 nm).

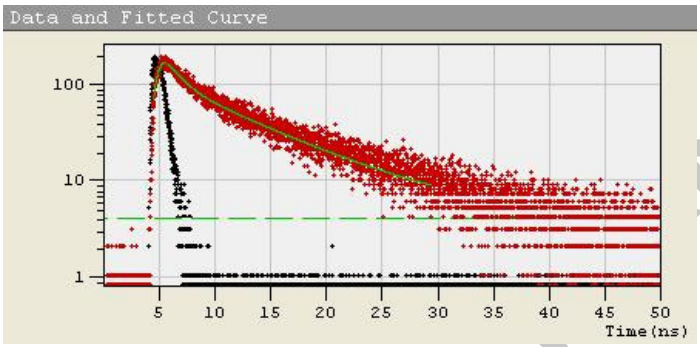

Figure S8: Time-resolved fluorescence decay of $\mathbf{L^2}$ (10^{-5} M in DMF) (ex = 300 nm).

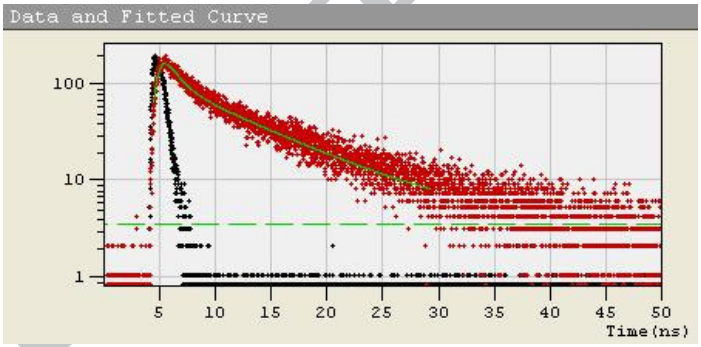

Figure S9: Time-resolved fluorescence decay of L^2-Fe^{3+} system (in DMF/water, 3:1,v/v) (ex = 300 nm).

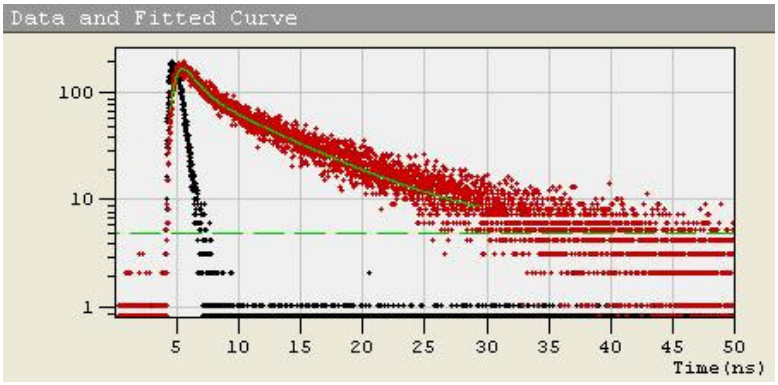

Figure S10: Time-resolved fluorescence decay of L^2-Cu^{2+} system (10^{-5} M in DMF/water, 3:1,v/v) (ex = 300 nm).

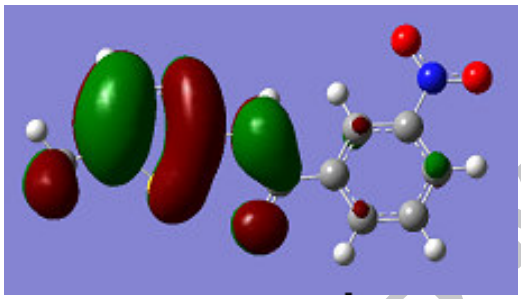

HOMO of the L^1

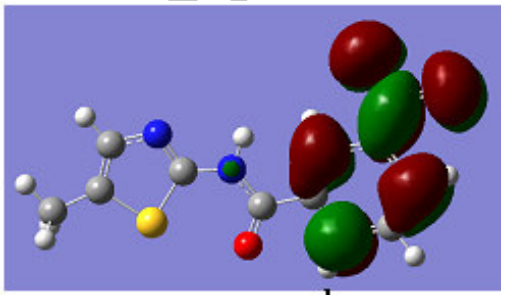

LUMO of the L^1

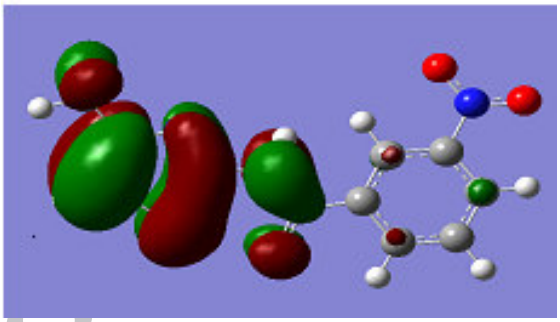

HOMO of the L^2

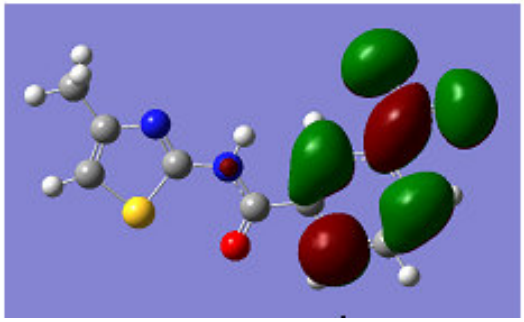

LUMO of the L^1

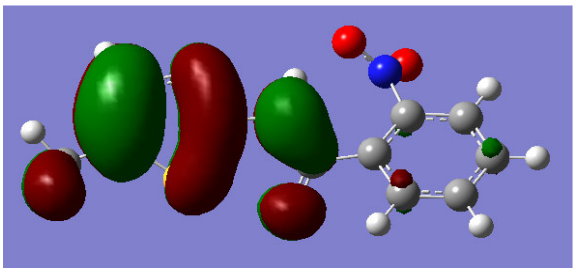

HOMO of the L^3

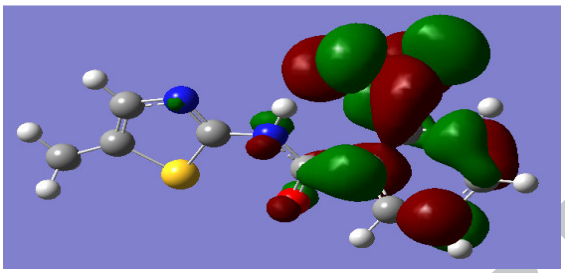

LUMO of the L^3

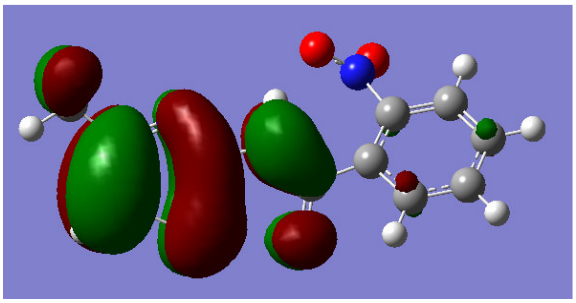

HOMO of the L^4

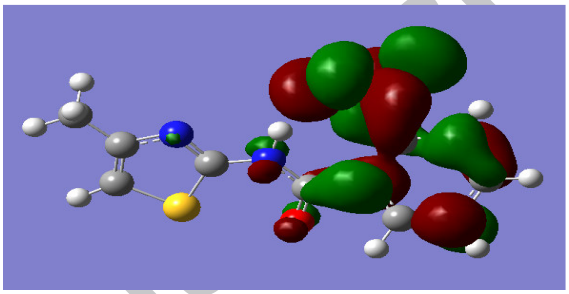

LUMO of the L^4

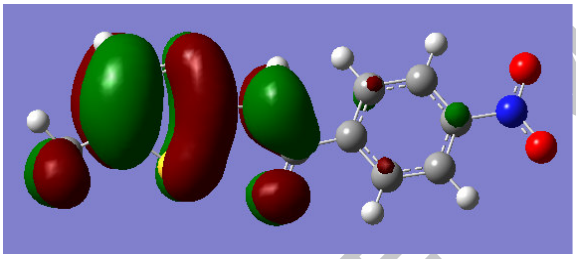

HOMO of the L^5

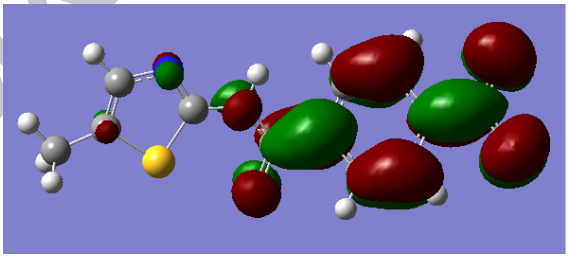

LUMO of the L^5

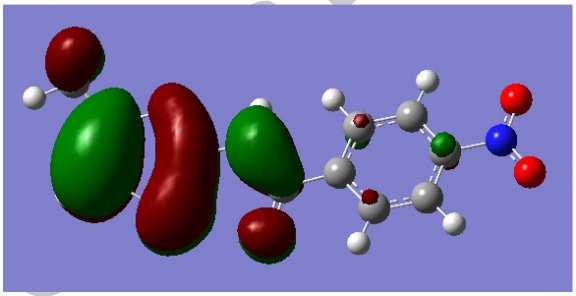

HOMO of the L^6

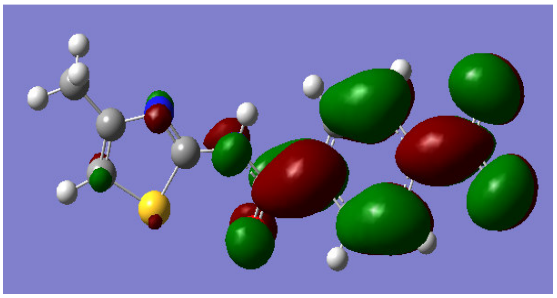

LUMO of the L^6

Figure S11: View of the HOMO and LUMO of $\mathbf{L^1}$-$\mathbf{L^6}$ from GaussView.

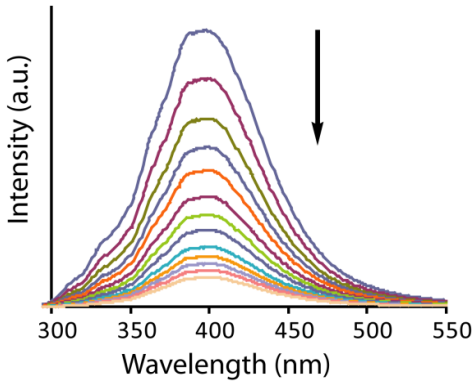

(a)

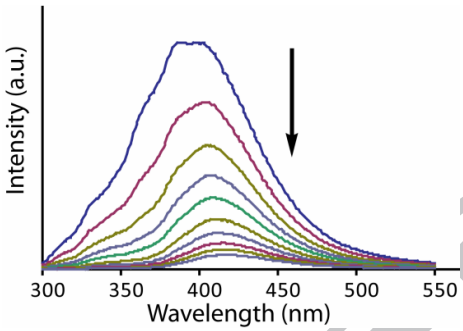

(b)

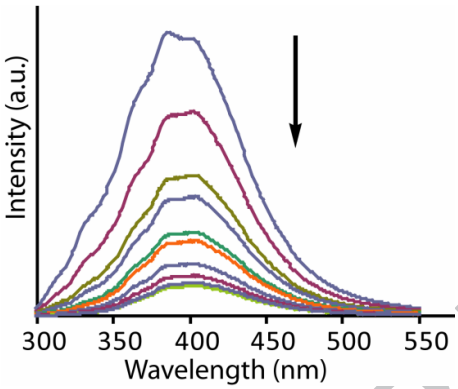

(c)

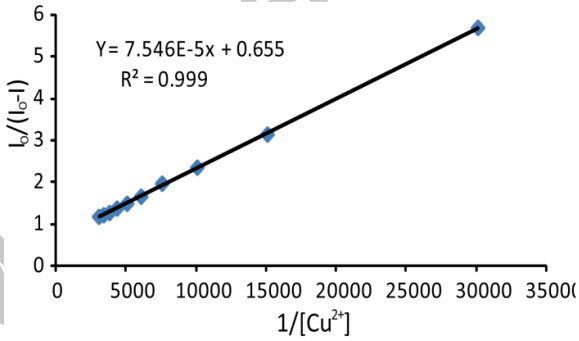

(d)

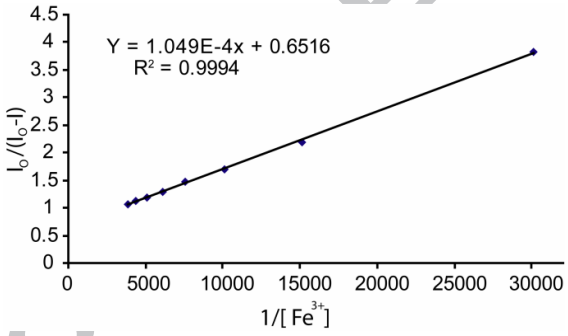

(e)

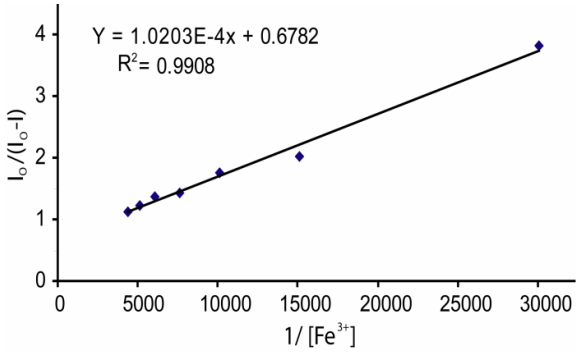

(f)

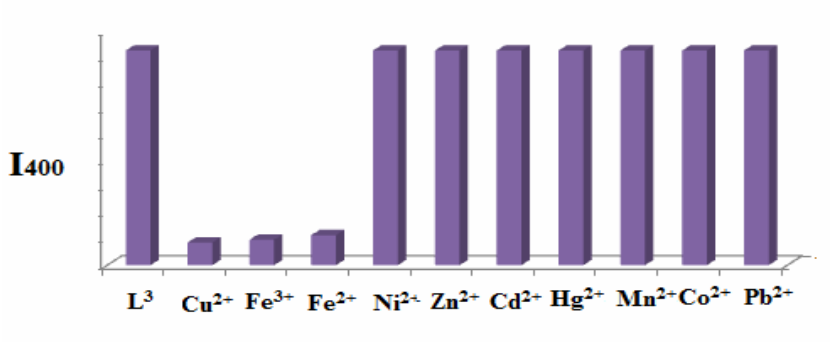

(g)

Figure S12: (a) Changes in fluorescence spectra of $\mathbf{L^3}$ in DMF/H_2O (3:1, 3 mL) upon addition of (a) Cu^{2+} ions (1×10^{-2} M) solution (b) Fe^{3+} ions (1×10^{-2} M) solution (c)) Fe^{2+} ions (1×10^{-2} M) solution by 10 µl in each aliquot. Binding constant determination of $\mathbf{L^3}$ (Benesi-Hildebrand plot) by fluorescence method with (d) Cu^{2+} (e) Fe^{3+} (f) Fe^{2+}. (g) The purple bars represent the intensity plot of $\mathbf{L^3}$ at λ= 400 nm with various metal ions.

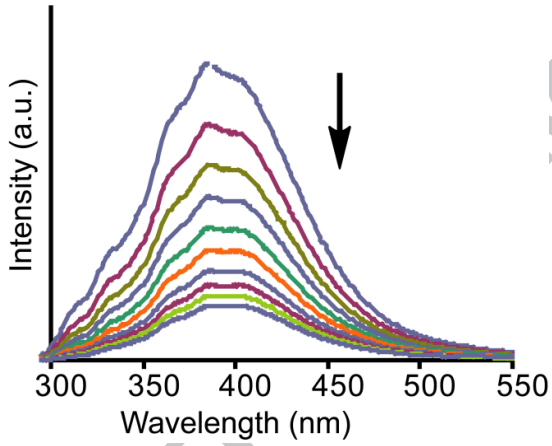

(a)

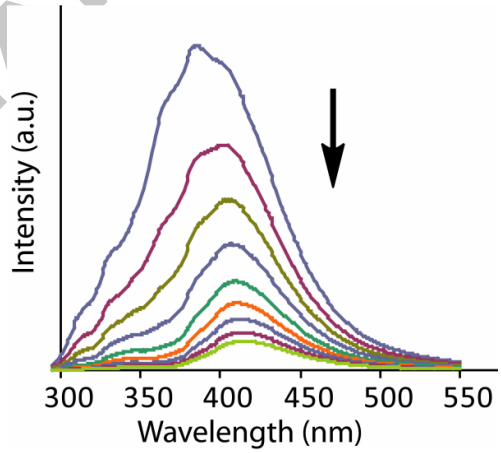

(b)

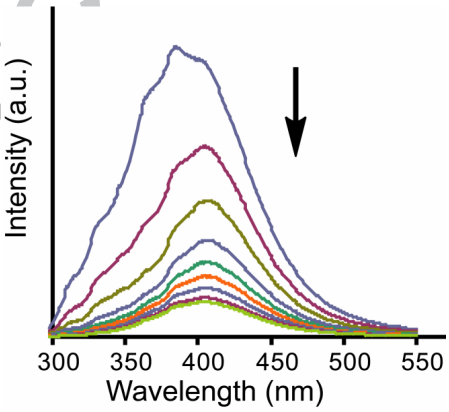

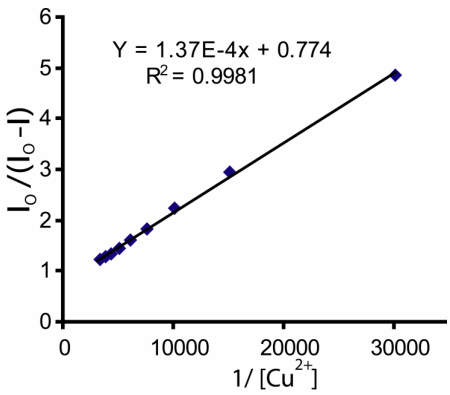

(c)

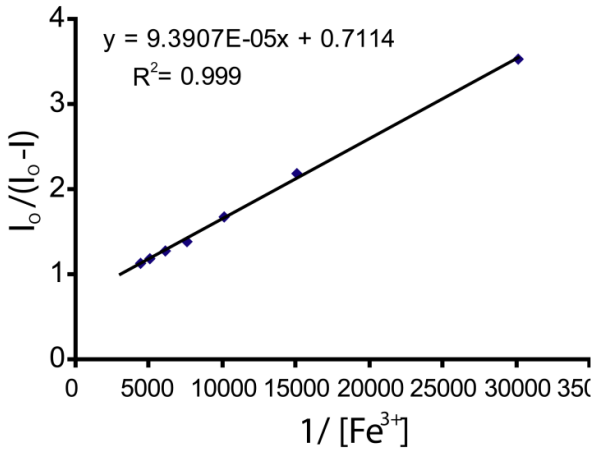

(d)

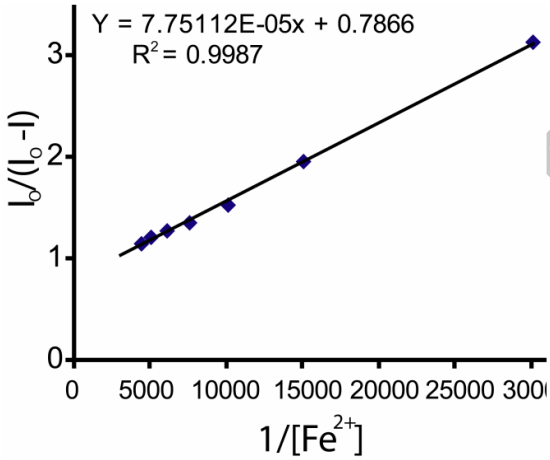

(e)

(f)

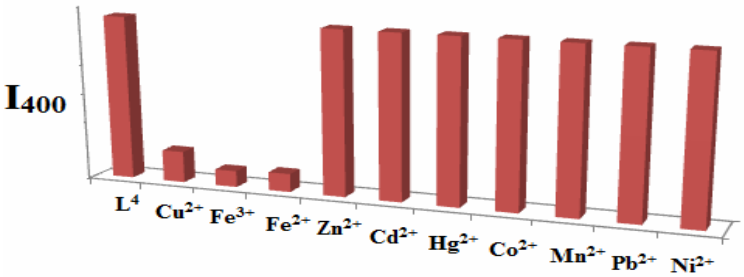

(g)

Figure S13: (a) Changes in fluorescence spectra of the **L**^{4} in DMF/H_2O (3:1, 3mL) upon addition of (a) Cu^{2+} ions (1×10^{-2} M) solution (b) Fe^{3+} ions (1×10^{-2} M) solution (c)) Fe^{2+} ions (1×10^{-2} M) solution by 10 µl in each aliquot. Binding constant determination of **L**^{4} (Benesi-Hildebrand plot) by fluorescence method with (d) Cu^{2+}, (e) Fe^{3+}, (f) Fe^{2+}. (g) The red bars represent the intensity plot of the **L**^{4} at λ= 400 nm with various metal ions.

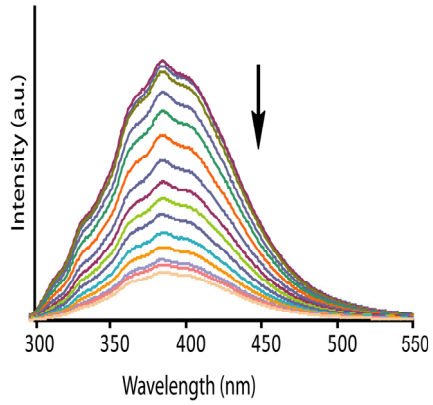
Intensity (a.u.)
300
350
400
450
500
550
Wavelength (nm)

(a)

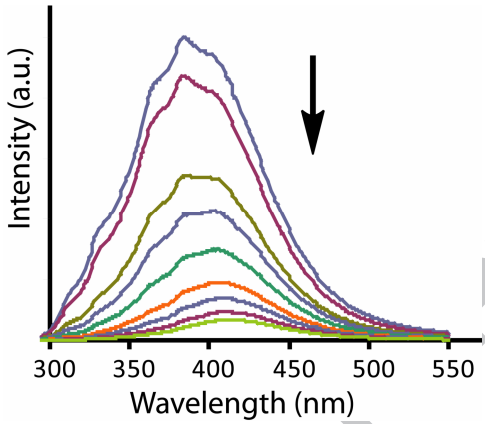
Intensity (a.u.)
300
350
400
450
500
550
Wavelength (nm)

(b)

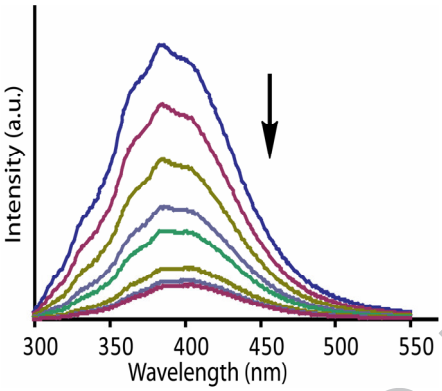
Intensity (a.u.)
300
350
400
450
500
550
Wavelength (nm)

(c)

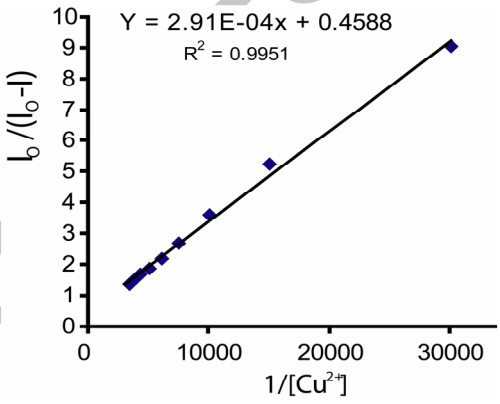
Y = 2.91E-04x + 0.4588
R2 = 0.9951
Io /(Io -I)
0
1
2
3
4
5
6
7
8
9
10
0
10000
20000
30000
1/[Cu2+]

(d)

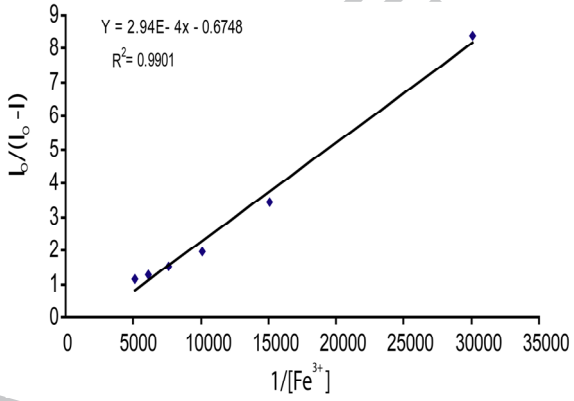
Y = 2.94E- 4x - 0.6748
R2= 0.9901
Io/(Io -I)
0
1
2
3
4
5
6
7
8
9
0
5000
10000
15000
20000
25000
30000
35000
1/[Fe3+]

(e)

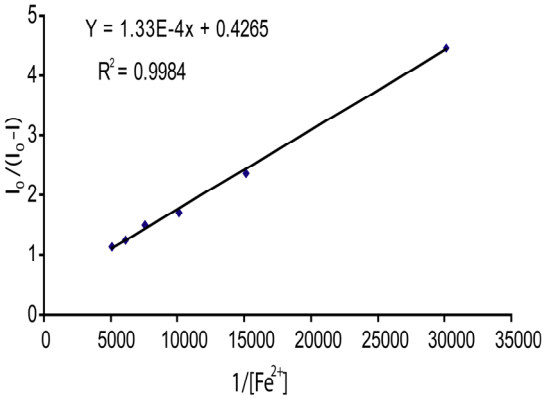
Y = 1.33E-4x + 0.4265
R2 = 0.9984
Io /(Io -I)
0
1
2
3
4
5
0
5000
10000
15000
20000
25000
30000
35000
1/[Fe2+]

(f)

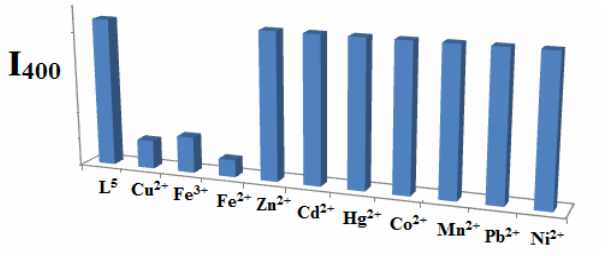

(g)

Figure S14: (a) Changes in fluorescence spectra of the $\mathbf{L^5}$ in DMF/H_2O (3:1, 3mL) upon addition of (a) Cu^{2+} ions (1 × 10^{-2} M) solution (b) Fe^{3+} ions (1×10^{-2} M) solution (c)) Fe^{2+} ions (1x10^{-2} M) solution by 10 µl in each aliquot. Binding constant determination of $\mathbf{L^5}$ (Benesi-Hildebrand plot) by fluorescence method with (d) Cu^{2+}, (e) Fe^{3+}, (f) Fe^{2+}. (g) The red bars represent the intensity plot of the $\mathbf{L^5}$ at λ= 400 nm with various metal ions.

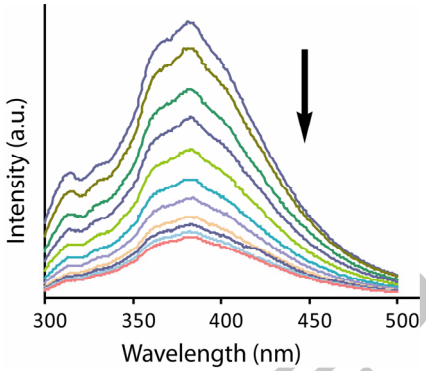

(a)

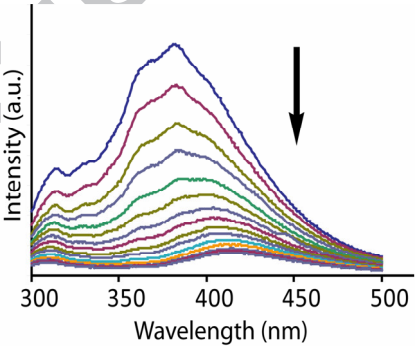

(b)

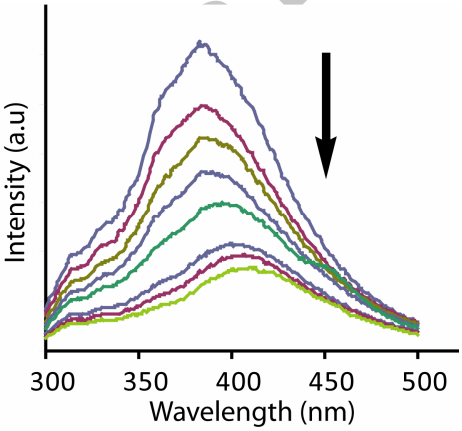

(c)

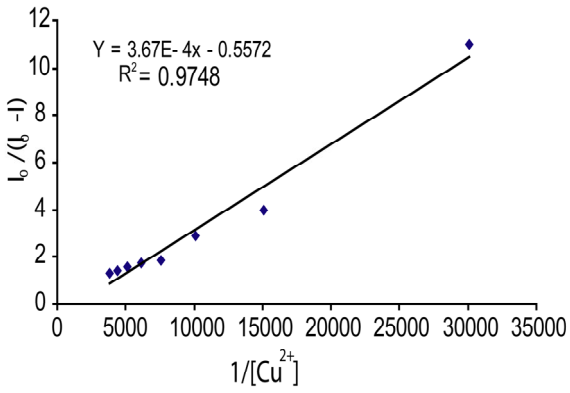

(d)

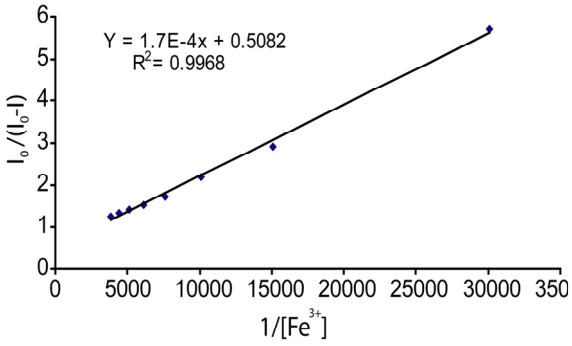

(e)

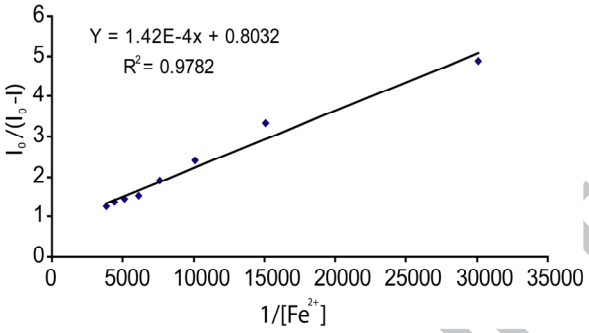

(f)

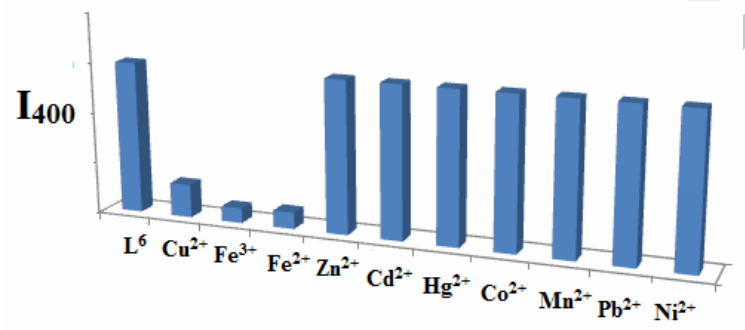

(g)

Figure S15: (a) Changes in fluorescence spectra of the **L**^{6} in DMF/H_2O (3:1, 3mL) upon addition of (a) Cu^{2+} ions (1×10^{-2} M) solution (b) Fe^{3+} ions (1×10^{-2} M) solution (c)) Fe^{2+} ions (1×10^{-2} M) solution by 10 µl in each aliquot. Binding constant determination of **L**^{6} (Benesi-Hildebrand plot) by fluorescence method with (d) Cu^{2+}, (e) Fe^{3+}, (f) Fe^{2+}. (g) The blue bars represents the intensity plot of the **L**^{6} at λ= 400 nm with various metal ions.

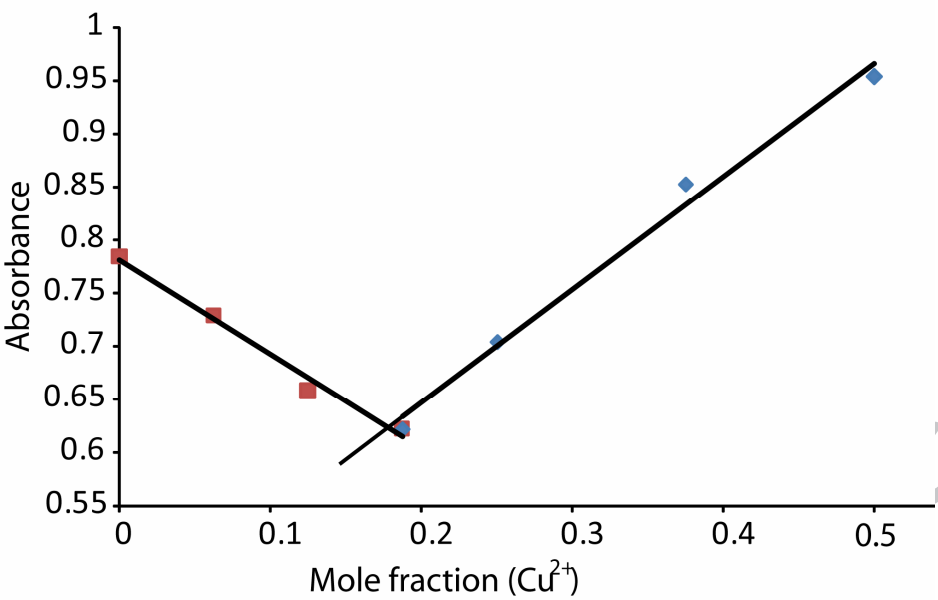

Figure S16: Job plot for binding of $\mathbf{L^1}$ with Cu^{2+}.

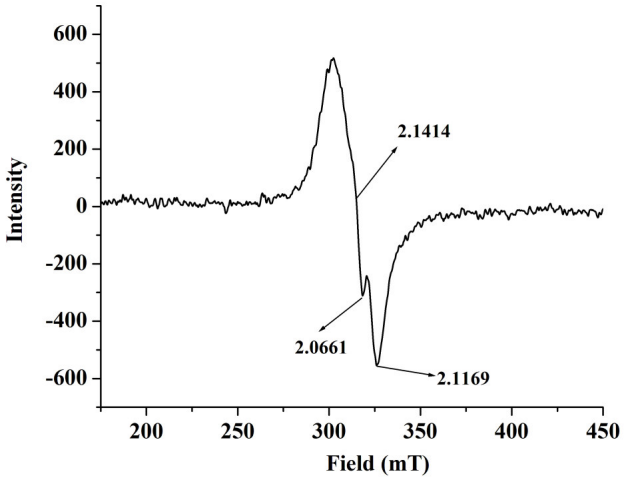

(a)

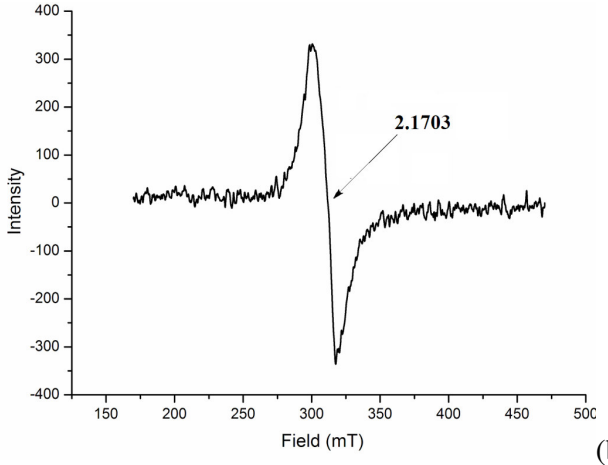

(b)

Figure S 17: (a) ESR spectra of a solution of equimolar solution of $\mathbf{L^1}$ cupric chloride in dimethylformamide solution. (b) ESR spectra of a solution of equimolar solution of $\mathbf{L^2}$ cupric chloride in dimethylformamide solution.

Table S1: Crystallographic parameters of the ligand $\mathbf{L^1}$

Compound No.	$\mathbf{L^1}$
Formulae	$C_{11}H_9N_3O_3S$
Mol. wt.	263.27
Crystal system	Monoclinic
Space group	$P\,2_1/n$
UTemperature (K)	296(2)
Wavelength (Å)	0.71073
a (Å)	3.9164(5)
b (Å)	13.1518(12)
c (Å)	22.183(3)
α (°)	90.00
β (°)	94.628(11)
γ (°)	90.00
V (Å^3)	1138.9(2)
Z	4
Density/g.cm^{-3}	1.535
Abs. Coeff. /mm^{-1}	0.288
Abs. Correction	multi-scan
F(000)	544
Total reflections	2008
Reflections, $I > 2\sigma(I)$	1164
Max. θ/°	25.00
Ranges (h, k, l)	-4 ≤ h ≤ 4 -9 ≤ k ≤15 -26 ≤ 1 ≤11
Complete to 2θ (%)	99.9
Data/ restrain/ parameter	2008/ 0/ 164
Goof(F^2)	1.005
R indices [$I > 2\sigma(I)$]	0.0594
R indices (all data)	0.1144

Distinctions of positional isomers of N-(methylthiazol-2-yl)nitrobenzamide by copper and iron ions

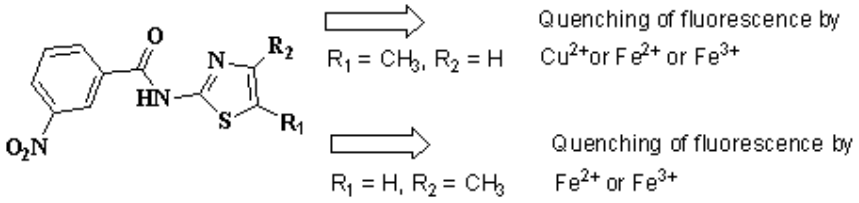

Fluorescence emission intensities of positional isomers of N-(methylthiazol-2-yl) nitrobenzamide were reduced by Cu^{2+}, Fe^{2+} and Fe^{3+} ions among a series of commonly abundant metal ions. One of the isomer showed an exceptional fluorescence decrease only in the presence of Fe^{2+} or Fe^{3+} ions making it distinguishable from other isomers in the series.

N. Phukan, A. Goswami, J. B. Baruah

Highlight:

Positional isomers of N-(methylthiazol-2-yl)nitrobenzamide show selective fluorescence responses to copper and iron ions.

One such positional isomer could be distinguished from the difference in emission changes with copper ions.

Electronic factors play an important role in the differentiation of fluorescence emission.